Springer

KSME

Journal of Mechanical Science and Technology 30 (2) (2016) 763~770
www.springerlink.com/content/1738-494x(Print)/1976-3824(Online)
DOI 10.1007/s12206-016-0131-8

Multi-objective collaborative optimization using linear physical programming with dynamic weight†

Haiyan Li[1,*], Mingxu Ma[2] and Wenlei Zhang[2]

[1]*School of Computer Science and Engineering, Northeastern University, Shenyang, 110819, China*
[2]*School of Mechanical Engineering and Automation, Northeastern University, Shenyang, 110819, China*

(Manuscript Received August 22, 2014; Revised May 22, 2015; Accepted October 7, 2015)

Abstract

The multi-objective collaborative optimization problem with multi-objective subsystems has a bi-level optimization architecture, that consists of the system and subsystem levels. Combining the multi-objective optimization algorithm with a bi-level optimization structure can obtain a satisfactory solution. Given that the preference-based algorithm requires minimal running time, the Linear physical programming (LPP) method, one of the typical preference-based algorithms, is adopted. Considering that setting the preference values for the incompatibility function is difficult, the weighted incompatibility function is added to the piecewise linear function of the LPP model. An expression of dynamic weight is also presented according to the inconsistency among the subsystems, which is caused by the sharing and auxiliary variables relative to the different subsystems. Using an engineering example, this study reveals that the interdisciplinary consistency is satisfactory when the dynamic weight is used in the LPP model, which thereby demonstrates the effectiveness of the presented method.

Keywords: Dynamic weight; Linear physical programming; Multi-disciplinary design optimization; Multi-objective collaborative optimization

1. Introduction

Multi-disciplinary design optimization (MDO), a tool of concurrent engineering for large-scale and complex system design, has gained considerable research attention and application [1]. The MDO methods are classified into single-level and multi-level methods. The single-level methods include simultaneous analysis and design, the multi-disciplinary feasible, and the individual discipline feasible. For complex coupling problems, the key approaches are the multi-level MDO methods that mainly include Collaborative optimization (CO), Concurrent subspace optimization (CSSO), bi-level integrated system synthesis, and analytical target cascading [2]. These MDO methods are mainly presented for single-objective MDO problems.

In many industrial environments, however, the engineering design of complex systems is inherently multi-disciplinary and multi-objective. Therefore, multi-objective optimization algorithms must be combined with these existing MDO methods. This characteristic increases the complexity to obtain a satisfactory solution. Hence, some studies have been conducted to effectively deal with multi-objective MDO problems. Researchers have paid attention to multi-objective CSSO [3, 4] and Multi-objective CO (MOCO) [5-15] and have made some important contributions to generating one Pareto solution. Other relevant multi-objective MDO methods, such as the multi-objective decomposition algorithm [16] and Pareto frontier analysis [17], are also developed.

Compared with other MDO methods, the CO method requires less information exchange among subsystems and allows more flexibility in subsystem optimization. Given the high degree of disciplinary autonomy, CO becomes an attractive method [18, 19]. The basic idea in the CO method is the decomposition of the design problem into two levels: the system and subsystem levels. The system level objective is minimized under the consistency requirements of the disciplines by enforcing equality constraints that coordinate interdisciplinary couplings.

The original CO method was presented for system design problems with a single-objective function at the system level, while the subsystems do not have any design objective [20]. Hence, some researchers have investigated the MOCO problems. For instance, Tappeta and Renaud [5] used the weighted-sum method to resolve the MOCO problem. A system-level objective function is formulated as the weighted sum of the subsystem-level objective functions. This formulation has the shortcomings of the weighting method. The goal

*Corresponding author. Tel.: +86 24 83687602, Fax.: +86 24 83687602
E-mail address: lihaiyan@mail.neu.edu.cn
† Recommended by Associate Editor Gil Ho Yoon

programming and Linear physical programming (LPP) approaches were also introduced to resolve the MOCO problems [6-8]. These MOCO frameworks allow designers to express their preferences for multiple conflicting objectives using physically meaningful parameters. Li et al. [9] adopted the LPP method in multi-objective subsystem optimization and transformed the incompatibility function into a disciplinary constraint to avoid providing preference values. Huang et al. [10] applied the fuzzy satisfaction degree and fuzzy sufficiency degree methods to address the MOCO problem. Their work provided a MOCO framework with the capability to handle fuzzy information. Li et al. [11] adopted the LPP method and the Non-dominated sorting in genetic algorithm (NSGA-II) at the multi-objective system and subsystem levels, respectively. They provided an interdisciplinary incompatibility function and physical objectives with different priority levels to avoid the difficulty in the process of NSGA-II. Vikrant and Shapour [12] used the Multi-objective genetic algorithm (MOGA) to solve the multi-objective optimization problems at the system and subsystem levels. Four strategies were provided to select a single solution from its Pareto set in each subsystem. Sébastien et al. [13] combined the MOGA with CO to address the MOCO problem using a "posteriori" choice. Hu et al. [14] adopted the genetic algorithm in system-level and subsystem-level problems and used the online approximation method to build meta-models for each subsystem.

The methods adopted in the above MOCO problems can be classified into two categories: the preference-based multi-objective optimization algorithm and the Multi-objective evolutionary algorithm (MOEA). The MOCO problems [5-10] using the preference-based multi-objective optimization algorithm need more preference information than the MOCO problems [11-14] using the MOEA method. However, the calculation efficiency of the former is higher than that of the latter. If the preference information is available, then the preference-based multi-objective optimization algorithm is a good choice for MOCO problems. Therefore, the LPP method, one of the typical preference-based algorithms, is adopted in this study.

In the original CO framework, the sole objective function in the subsystem is to minimize the incompatibility function [7]. Hence, subsystem optimization is not related to physical objectives and aims to minimize interdisciplinary incompatibilities. However, studies on MOCO problems with physical objectives in subsystem is important because a subsystem instead of the system level sometimes involves one or more physical objectives. For example, in the design of an aircraft, the wing subsystem has weight and deflection as physical objectives, whereas the system level has total weight and stress as the system-level objectives [15]. MDO problems with multi-objective subsystems are really involved in some engineering problems.

Previous works have paid rare attention to the multi-objective subsystem [5-15]. Therefore, this study investigates the MOCO problem with multi-objective subsystems, while the LPP method is adopted in the multi-objective subsystem. The contributions of this study concentrate on two aspects. First, the weighted incompatibility function is added to the piecewise linear function of the LPP model in the multi-objective subsystem. This proposed method can avoid the difficulty in setting the ranges of desirability for the incompatibility function when the preference-based multi-objective optimization algorithm is adopted. Second, a reasonable dynamic weight for the incompatibility function is presented according to the inconsistency among the subsystems. The value of the incompatibility function gradually tends to zero as the bi-level optimization proceeds, which leads to the difficulty in setting an ideal fixed weight. Therefore, this proposed dynamic weight is necessary.

2. Formulation of CO with multi-objective subsystems

The CO proposed by Kroo et al. [20] is a bi-level optimization architecture that consists of the system and subsystem levels. The system-level optimizer minimizes the overall objective function subject to the interdisciplinary compatibility constraints obtained from the optimization results of the subsystem level. The action of the system-level optimization is to determine the target values for the subsystem level. The subsystem-level optimizer minimizes the incompatibility function subject to the disciplinary constraints.

The system level attempts to optimize the design objective function F subject to n interdisciplinary compatibility constraints J_i^*.

$$\begin{aligned} &\min F(z) \\ &\text{s.t. } J_i^*(z, \boldsymbol{x}_i^*(z)) = 0,\ i = 1,2,\cdots,n, \end{aligned} \tag{1}$$

where $\boldsymbol{x}_i^*(z)$ (i.e., the optimal value of the subsystem i) is the function with respect to the system-level design vector $\boldsymbol{z}$. An overall compatibility constraint was introduced in the system level by Li et al. [9] to decrease the influence on the optimization result caused by the starting point.

In the multi-objective subsystem level, the objective functions include physical objectives, aside from the incompatibility function, which is the sole objective function in the original CO framework. The expression of the multi-objective subsystem i is then given as follows:

$$\min J_i(\boldsymbol{x}_i) = \sum_{j=1}^{s_i} (x_{ij} - z_j^*)^2, \tag{2}$$

$$\begin{aligned} &\min \left\{ f_{i1}(\boldsymbol{x}_i), f_{i2}(\boldsymbol{x}_i), \cdots, f_{in_s}(\boldsymbol{x}_i) \right\} \\ &\text{s.t. } c_i(\boldsymbol{x}_i) \le 0, \end{aligned} \tag{3}$$

where $J_i(\boldsymbol{x}_i)$ is the incompatibility function of the subsystem i, s_i is the number of the sharing and auxiliary variables, $f_{i1}(\boldsymbol{x}_i) \sim f_{in_s}(\boldsymbol{x}_i)$ denote the physical objectives of the subsystem i, in_s denotes the number of physical objectives, z_j^* is the jth target value allocated by the system level, and $c_i(\boldsymbol{x}_i)$ is the

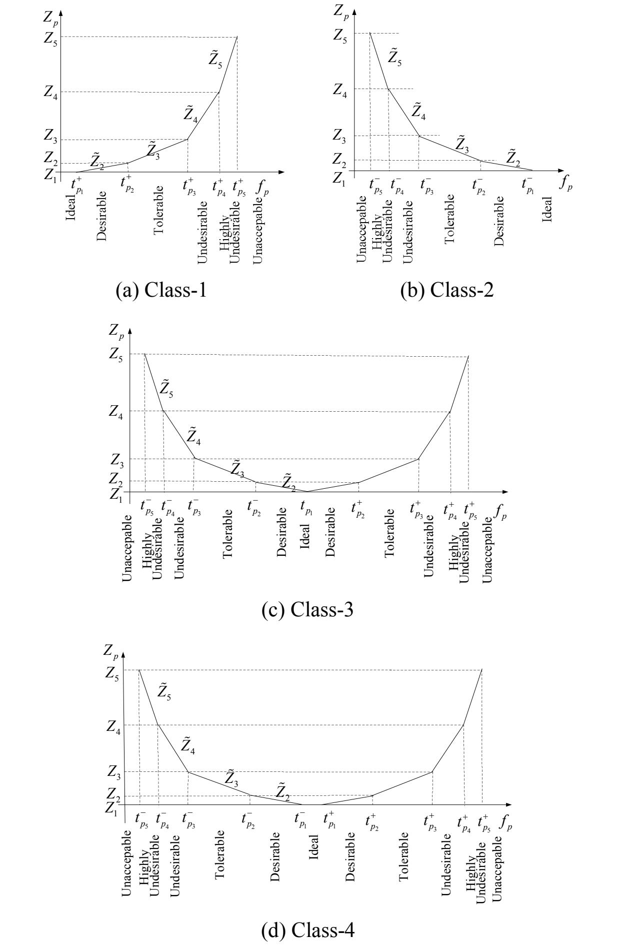

Fig. 1. LPP class function regions.

disciplinary constraint.

3. Multi-objective subsystem optimization

The LPP is one of the typical preference-based algorithms that require less running time than the MOEA method. For smoothness of performance and convenience in this study, we concentrate on the LPP for the multi-objective subsystem optimization.

3.1 LPP description

LPP is an engineering method that addresses multi-objective optimization problems using the preference of the designer [21]. With the LPP procedure, the designer expresses his/her preference with respect to each criterion using the following four different classes: (i) Smaller-Is-Better (1S), (ii) Larger-Is-Better (2S), (iii) Value-Is-Better (3S), and (iv) Range-Is-Better (4S). Fig. 1 presents the depiction. Z_p is the class function that is smaller-better to each class. f_p is the value of the criterion under consideration.

The designer should decide which class to adopt and select the range targets (i.e., $t_{p1}^{+} \sim t_{p5}^{+}$). Given that decisions are made in a multi-objective environment, an implicit or explicit inter-criterion preference should be provided, which is guaranteed with the One vs. Others rule [21].

3.2 Formulation of the weighted LPP model

Considering that LPP is a preference-based algorithm, we should set the ranges of desirability for all the objective functions. The incompatibility function is used to make the optimal value match the target value allocated by the system level as closely as possible, the value of which gradually tends to zero as the bi-level optimization proceeds. Given that setting the ranges of the desirability of the incompatibility function is difficult, the weighted incompatibility function is added to the piecewise linear function of the LPP model. The formulation of the LPP model is then given as follows:

$$\min \tilde{J}_i = \sum_{p=1}^{n_s}\sum_{s=2}^{5}(\tilde{w}_{ps}^{-}d_{ps}^{-} + \tilde{w}_{ps}^{+}d_{ps}^{+}) + \gamma(J_i(\boldsymbol{x}_i)) \tag{4}$$

s.t. $f_{ip}(\boldsymbol{x}_i) - d_{ps}^{+} \le t_{p(s-1)}^{+}$, $f_{ip}(\boldsymbol{x}_i) \le t_{p5}^{+}$, $d_{ps}^{+} \ge 0$

(Classes 1S, 3S, 4S)

$f_{ip}(\boldsymbol{x}_i) + d_{ps}^{-} \ge t_{p(s-1)}^{-}$, $f_{ip}(\boldsymbol{x}_i) \ge t_{p5}^{-}$, $d_{ps}^{-} \ge 0$

(Classes 2S, 3S, 4S)

$c_i(\boldsymbol{x}_i) \le 0$,

where n_s denotes the number of physical objectives, d_{ps}^{-} denotes the negative deviation value between f_{ip} and $t_{p(s-1)}^{-}$, and d_{ps}^{+} denotes the positive deviation value between f_{ip} and $t_{p(s-1)}^{+}$. The calculation process of the weight $\tilde{w}_{ps}^{-}$ and $\tilde{w}_{ps}^{+}$ is given in Ref. [21].

3.3 Setting of dynamic weight

The value of J_i in Eq. (4) gradually tends to zero as the bi-level optimization proceeds. Therefore, an ideal fixed weight γ is difficult to obtain. Instead, a dynamic weight γ is built using the inconsistency among the subsystems. The expression is given as

$$\gamma = \alpha\left(\frac{1}{10^{\mu}k + \varepsilon} + 10^{\mu}k\right), \tag{5}$$

where k denotes the inconsistency among the subsystems, and μ and ε are given by the designer. The values of these parameters are set as follows:

(1) μ: Its value is given according to the requirements of interdisciplinary consistency. The initial value of μ can usually be set using the final accuracy of the inconsistency among the subsystems. For example, assuming that the final accuracy of the inconsistency among the subsystems is $k_t = 10^{-\tau}$, the initial value of μ can be $\mu = -\log_{10}k_t = \tau$. If the final interdisciplinary consistency is not satisfactory, then we can set $\mu := \mu + 1$.

(2) ε: In the late stage of bi-level optimization, the value of $10^{\mu}k$ may be small. In this case, the value of ε can control the maximum value of $\frac{1}{10^{\mu}k+\varepsilon}$ to prevent γ from being too large, that is, if $10^{\mu}k \to 0$, then $\gamma \approx \frac{1}{\varepsilon}$. Therefore, the value of ε is usually a small positive value, such as 0.01 and 0.001.

(3) α: If the initial value of k is large, $10^{\mu}k$ may increase the value of γ. The factor α can avoid a too large value of γ. Given that k takes a large value only at the earlier stage of bi-level optimization, the value of α on (0, 1] increases as the iteration number increases. The expression is given as

$$\alpha = 10^{(\frac{ss_i - 1}{ss_n} - 1)\mu}, \tag{6}$$

where ss_i denotes the current iteration number of bi-level optimization, and ss_n denotes the estimated value of the maximum iteration number.

At the first iteration (i.e., ss_i = 1), the value of weight γ is given by

$$\begin{aligned}\gamma_0 &= \alpha(\frac{1}{10^{\mu}k+\varepsilon} + 10^{\mu}k) \\ &= (10^{(\frac{1-1}{ss_n}-1)\mu})(\frac{1}{10^{\mu}k+\varepsilon} + 10^{\mu}k) = 10^{-\mu}(\frac{1}{10^{\mu}k+\varepsilon} + 10^{\mu}k)\end{aligned}. \tag{7}$$

If the initial value of k is large, then the initial value of weight γ is obtained as follows:

$$\gamma_0 = 10^{-\mu}(\frac{1}{10^{\mu}k+\varepsilon} + 10^{\mu}k) \approx 10^{-\mu}(0 + 10^{\mu}k) = k\ . \tag{8}$$

In the last iteration (i.e., $ss_i = ss_n$), the value of weight γ is given by

$$\begin{aligned}\gamma_{final} &= \alpha(\frac{1}{10^{\mu}k+\varepsilon} + 10^{\mu}k) = (10^{(\frac{ss_n-1}{ss_n}-1)\mu})(\frac{1}{10^{\mu}k+\varepsilon} + 10^{\mu}k) \\ &\approx \frac{1}{10^{\mu}k+\varepsilon} + 10^{\mu}k.\end{aligned} \tag{9}$$

4. Parameter design of rolling mill stand

The parameter design of the rolling mill stand is modeled as an MDO problem [9, 22, 23] with multi-objective subsystems. The formulation is given as follows:

$$f_1(\boldsymbol{x}) = 1.91\times10^{-6}\times(x_1+0.59)^3\times(\frac{1}{x_4x_3^3}+\frac{1}{x_6x_5^3}) \left\{1-\frac{3}{4}\times\left[1+\frac{(x_3+x_5+4.3)x_4x_2^3x_6x_5^3}{(x_1+0.59)x_2x_1^3(x_4x_3^3+x_6x_5^3)}\right]^{-1}\right\}, \tag{10}$$

$$f_2(\boldsymbol{x}) = 3.704\times10^{-6}\times(x_1+0.59)\times(\frac{1}{x_3x_4}+\frac{1}{x_5x_6}), \tag{11}$$

$$f_3(\boldsymbol{x}) = 5.119\times10^{-6}\times\frac{1}{x_1x_2}, \tag{12}$$

$$\begin{aligned}f_4(\boldsymbol{x}) = 0.9671\times10^{-6}\times[&8(x_2+0.656)^3-0.64(x_2+\\ &0.656)+0.064+8(x_2+0.256)^3\times\\ &(218.8x_7^4-1)]/x_7^4\end{aligned}, \tag{13}$$

$$\begin{aligned}f_5(\boldsymbol{x}) = 1.533\times10^{-5}\times[&(x_2+0.656)-0.2+(x_2+\\ &0.256)\times(14.79x_7^2-1)]/x_7^2\end{aligned}, \tag{14}$$

$$f_6(\boldsymbol{x}) = 0.263\times10^{-4}\ln\left[0.5904\times10^5\times(x_7+0.28)\right], \tag{15}$$

$$\begin{aligned}f_7(\boldsymbol{x}) = 15.6\times[&2.15x_1x_2+\\ &(x_3x_4+x_5x_6)(x_1+0.295)]\end{aligned}, \tag{16}$$

$$\begin{aligned}
\text{s.t.}\quad & g_1(\boldsymbol{x}) = x_7 - 0.42 \le 0\\
& g_2(\boldsymbol{x}) = 0.336 - x_7 \le 0\\
& g_3(\boldsymbol{x}) = 0.829\times10^6\times\sqrt{1+0.28/x_7} - 1.61\times10^6 \le 0\\
& g_4(\boldsymbol{x}) = 0.1678\times10^6\times(x_2+0.256) - 0.125\times10^6 \le 0\\
& g_5(\boldsymbol{x}) = \frac{500}{x_1x_2} + \frac{750(x_1+0.59)}{x_1^2x_2}\times\\
& \qquad \frac{1}{\left[1+\frac{(x_3+x_5+4.3)x_4x_3^3x_6x_5^3}{(x_1+0.59)x_2x_1^3(x_4x_3^3+x_6x_5^3)}\right]} - 0.055\times10^6 \le 0\\
& g_6(\boldsymbol{x}) = \frac{1.5\times10^3(x_1+0.59)}{x_4x_3^2}\times\\
& \qquad \left\{1-\frac{1}{2\left[1+\frac{(x_3+x_5+4.3)x_4x_3^3x_6x_5^3}{(x_1+0.59)x_2x_1^3(x_4x_3^3+x_6x_5^3)}\right]}\right\} -\\
& \qquad 0.055\times10^6 \le 0\\
& g_7(\boldsymbol{x}) = \frac{1.5\times10^3(x_1+0.59)}{x_6x_5^2}\times\\
& \qquad \left\{1-\frac{1}{2\left[1+\frac{(x_3+x_5+4.3)x_4x_3^3x_6x_5^3}{(x_1+0.59)x_2x_1^3(x_4x_3^3+x_6x_5^3)}\right]}\right\} -\\
& \qquad 0.055\times10^6 \le 0\\
& g_8(\boldsymbol{x}) = x_2 - x_1 \le 0\\
& g_9(\boldsymbol{x}) = x_4 - x_3 \le 0\\
& g_{10}(\boldsymbol{x}) = x_6 - x_5 \le 0\\
& g_{11}(\boldsymbol{x}) = 0.26 - x_2 \le 0\\
& g_{12}(\boldsymbol{x}) = -x_4 \le 0\\
& g_{13}(\boldsymbol{x}) = -x_6 \le 0\\
& g_{14}(\boldsymbol{x}) = x_3 - 2.5x_4 \le 0\\
& g_{15}(\boldsymbol{x}) = x_5 - 2.5x_6 \le 0\\
& g_{16}(\boldsymbol{x}) = 15.6\times\left[2.15x_1x_2 + (x_1+0.295)(x_3x_4+x_5x_6)\right] -\\
& \qquad 7.484 \le 0
\end{aligned}$$

where $x_1(h_1)$ and $x_2(b_1)$ are the height and width of the cross-section of the column, respectively; $x_3(h_2)$ and $x_4(b_2)$ are the height and width of the cross section of the upper beam, respectively; $x_5(h_3)$ and $x_6(b_3)$ are the height and width of the cross section of the lower beam, respectively; and $x_7(D_1)$ is the diameter of the backup roll. The diagram of the simplified rolling mill stand is given in Fig. 2.

The core goal of the problem is to optimize the stiffness of the rolling mill stand, which can been represented by the following seven objective functions: the sum of the bending deflection caused by the bending moment of the upper and lower beams (f_1), the sum of the bending deflection caused by the shearing force of the upper and lower beams (f_2), the tensile deformation of the column (f_3), the sum of the bending deflection caused by the bending moment of the backup roll (f_4), the sum of the bending deflection caused by the shearing force of the backup roll (f_5), the sum of the elastic flattening between the working roll and backup roll (f_6), and the weight of the stand (f_7). In addition, the design is subject to 16 inequality constraints. The constraints are the diameter restrictions of the backup roll body (g_1 and g_2), the contact strength restriction of the roll (g_3), the bending strength restriction of the dangerous section of the roll neck on the juncture of the body and neck of the backup roll (g_4), the composite strength restriction of the bending and tensile strengths of the column (g_5), the bending strength restrictions of the upper and lower beams (g_6 and g_7), the geometric restrictions of the column and beam (g_8-g_{15}), and the weight restriction of the stand (g_{16}).

The decomposed formulation consists of one system-level subproblem (i.e., weight) and three subsystem-level subproblems (i.e., column, beam, and backup roll). The objective in the system-level subproblem is to minimize objective f_7. The column subproblem is to minimize objective f_3 with constraints g_5, g_8, and g_{11}. The beam subproblem is to minimize objectives f_1 and f_2 with constraints g_6, g_7, g_9, g_{10}, and g_{12}-g_{15}. The backup roll subproblem is to minimize objectives f_4, f_5, and f_6 with constraints g_1-g_4. The expressions are given below.

System-level optimization:

$$\begin{aligned} &\min\ F(z)=f_7(z) \\ &\text{s.t. } J_1^*(\mathbf{z})=(z_1-x_{11}^*)^2+(z_2-x_{12}^*)^2+(z_3-x_{13}^*)^2+ \\ &\qquad (z_4-x_{14}^*)^2+(z_5-x_{15}^*)^2+(z_6-x_{16}^*)^2=0 \\ &\quad J_2^*(\mathbf{z})=(z_1-x_{21}^*)^2+(z_2-x_{22}^*)^2+(z_3-x_{23}^*)^2+ \\ &\qquad (z_4-x_{24}^*)^2+(z_5-x_{25}^*)^2+(z_6-x_{26}^*)^2=0 \\ &\quad J_3^*(\mathbf{z})=(z_2-x_{31}^*)^2+(z_7-x_{32}^*)^2=0 \end{aligned} \quad (17)$$

Subsystem optimization of the column:

$$\min f_{11}(\boldsymbol{x}_1)=(x_{11}-z_1^*)^2+(x_{12}-z_2^*)^2+(x_{13}-z_3^*)^2+(x_{14}-z_4^*)^2+(x_{15}-z_5^*)^2+(x_{16}-z_6^*)^2 \quad (18)$$

$$\min f_{12}(\boldsymbol{x}_1)=f_3(\boldsymbol{x}_1) \quad (19)$$

$$\text{s.t. } g_j(\boldsymbol{x}_1)\le 0,\quad j=5,8,11.$$

Subsystem optimization of the beam:

$$\min f_{21}(\boldsymbol{x}_2)=(x_{21}-z_1^*)^2+(x_{22}-z_2^*)^2+(x_{23}-z_3^*)^2+(x_{24}-z_4^*)^2+(x_{25}-z_5^*)^2+(x_{26}-z_6^*)^2 \quad (20)$$

Table 1. Desirable ranges of each criterion for the beam and backup roll disciplines.

Objective	f_1 (mm)	f_2 (mm)	f_4 (mm)	f_5 (mm)	f_6 (mm)
t_{p1}^+	0.0100	0.0100	0.1500	0.0500	0.1000
t_{p2}^+	0.0253	0.0309	0.3000	0.1200	0.2200
t_{p3}^+	0.0278	0.0367	0.4900	0.1500	0.2900
t_{p4}^+	0.0400	0.0500	0.5400	0.2000	0.3500
t_{p5}^+	0.0550	0.0600	0.6500	0.2500	0.4500

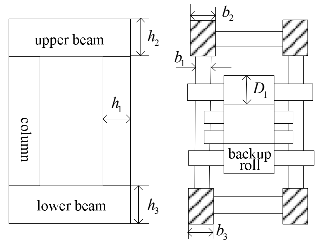

Fig. 2. Diagram of the simplified stand.

$$\min f_{22}(\boldsymbol{x}_2)=f_1(\boldsymbol{x}_2) \quad (21)$$

$$\min f_{23}(\boldsymbol{x}_2)=f_2(\boldsymbol{x}_2) \quad (22)$$

$$\text{s.t. } g_j(\boldsymbol{x}_2)\le 0,\quad j=6,7,9,10,12,13,14,15.$$

Subsystem optimization of the backup roll:

$$\min f_{31}(\boldsymbol{x}_3)=(x_{31}-z_2^*)^2+(x_{32}-z_7^*)^2 \quad (23)$$

$$\min f_{32}(\boldsymbol{x}_3)=f_4(\boldsymbol{x}_3) \quad (24)$$

$$\min f_{33}(\boldsymbol{x}_3)=f_5(\boldsymbol{x}_3) \quad (25)$$

$$\min f_{34}(\boldsymbol{x}_3)=f_6(\boldsymbol{x}_3) \quad (26)$$

$$\text{s.t. } g_j(\boldsymbol{x}_3)\le 0,\quad j=1,2,3,4.$$

The Class-1 of the LPP method is adopted for the multi-objective subsystem optimization. The dynamic weighted incompatibility function is added to the piecewise linear function of the LPP model. The preference values of the physical objectives are listed in Table 1 with the data provided by Cui [22].

4.1 Analysis of the interdisciplinary consistency

On the one hand, the interdisciplinary consistency is the most important property of the MDO algorithm. On the other hand, the proposed dynamic weight of the incompatibility function in the LPP model affects the interdisciplinary consistency. Therefore, the interdisciplinary consistency is an important factor.

The inconsistency among the subsystems is expressed by

$$k=J_1(\boldsymbol{x}_1^*,z_1^*)+J_2(\boldsymbol{x}_2^*,z_2^*)+J_3(\boldsymbol{x}_3^*,z_3^*), \quad (27)$$

where $\boldsymbol{z}_1^*$-$\boldsymbol{z}_3^*$ are the target values allocated by the system level. $\boldsymbol{x}_1^*$-$\boldsymbol{x}_3^*$ are the optimal values of the subsystems.

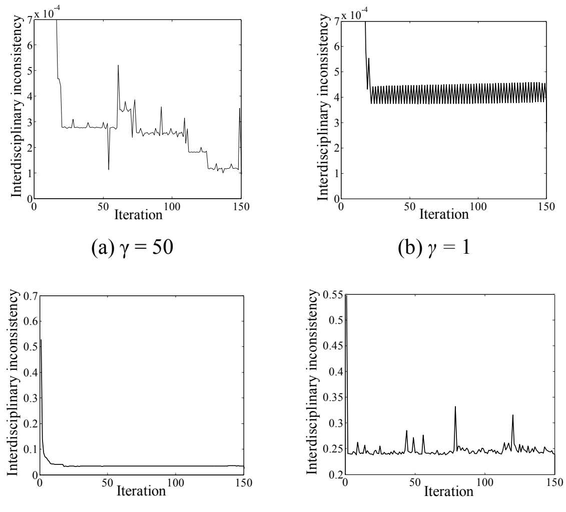

(a) γ = 50 (b) γ = 1

(c) γ = 0.01 (d) γ = 0.001

Fig. 3. Inconsistency among the subsystems from the fixed weight.

The initial target value allocated by the system level is z0 = [0,0,0,0,0,0,0]. In the piecewise linear function of the LPP model, the fixed and dynamic weights are both adopted to illustrate the effectiveness of the proposed dynamic weight.

Given the small magnitudes of the piecewise linear function and the incompatibility function, the value of the fixed weight should be small. Figs. 3(a)-(d) show the convergence curves for the inconsistency among the subsystems when the values of the fixed weight are 50, 1, 0.01 and 0.001, respectively.

The results in Figs. 3(c) and (d) present that the values of interdisciplinary inconsistency obtained with γ = 0.01 and 0.001 cannot be treated as zero, which indicate that the interdisciplinary consistency is not satisfactory. The too small weight of the incompatibility function in the LPP model may lead to a large value of the incompatibility function, which causes an unsatisfactory interdisciplinary consistency.

The results presented in Figs. 3(a) and (b) imply that the values of interdisciplinary inconsistency obtained with γ = 50 and 1 can be treated as zero, which indicate that the interdisciplinary consistency is satisfactory. However, the convergence curve of interdisciplinary inconsistency has a jitter. When the weight of the incompatibility function in the LPP model is too large, the optimizer of MATLAB may cause this jitter.

A reasonable weight in the LPP model is difficult to determine because the value of the incompatibility function gradually tends to zero as the bi-level optimization proceeds.

The proposed dynamic weight is then used in the LPP model. The value of ε in Eq. (5) is set ε = 0.001. Figs. 4(a)-(d) show the convergence curves for the inconsistency among the subsystems when the values of μ in Eq. (5) are 4, 5, 6 and 7, respectively.

The convergence curves of the inconsistency among the subsystems in Figs. 4(a)-(d) are better than those presented in Fig. 3. The expression of the dynamic weight is built with the inconsistency among the subsystems, and the extremum of the

Table 2. Design of the initial points.

Initial point	1	2	3	4
x_1(m)	0.0000	1.0000	0.5000	0.0800
x_2(m)	0.0000	1.0000	1.0000	0.2600
x_3(m)	0.0000	1.0000	0.5000	0.0800
x_4(m)	0.0000	1.0000	1.0000	0.0800
x_5(m)	0.0000	1.0000	0.5000	0.0800
x_6(m)	0.0000	1.0000	1.0000	0.0800
x_7(m)	0.0000	1.0000	0.5000	0.4095

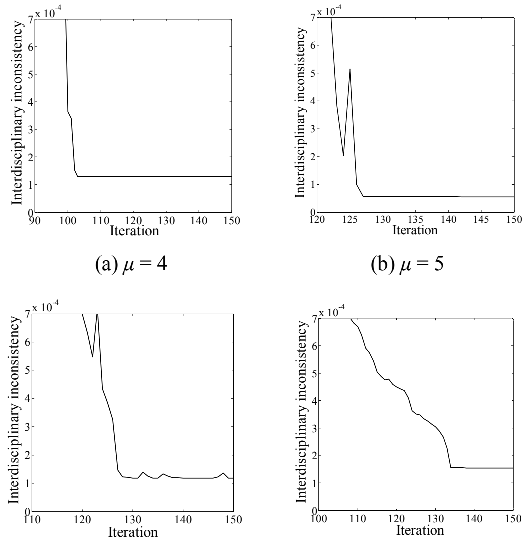

(a) μ = 4 (b) μ = 5

(c) μ = 6 (d) μ = 7

Fig. 4. Inconsistency among the subsystems from the dynamic weight.

dynamic weight is controlled in its expression. Therefore, the convergence curves of the interdisciplinary inconsistency obtained from the dynamic weight are better than those obtained from the fixed weight.

The values of the interdisciplinary inconsistency obtained from the dynamic weight are rounded to 10^{-4}, which can be treated as zero. Therefore, the interdisciplinary consistency is satisfactory when the dynamic weight is used in the LPP model. The accuracy of interdisciplinary consistency may be affected by the optimization toolbox and the optimization algorithm.

4.2 Analysis of the system-level optimization

The four initial points listed in Table 2 are selected as the target points allocated by the system level. The experimental data and analysis [24, 25] imply that CO obtains different solutions from several initial points. This phenomenon indicates that CO is sensitive to the initial point for some problems. Li et al. [9] introduced an overall compatibility constraint into the system-level optimization to reduce the influence of the initial point on the optimization result. In this study, the overall compatibility constraint is also adopted for this MOCO

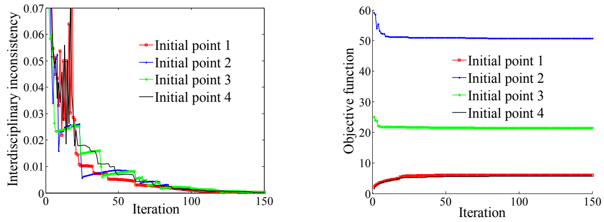

(a) Inconsistency among the subsystems (b) Objective function

Fig. 5. Results obtained from the dynamic weight.

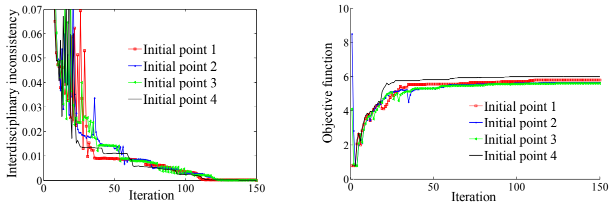

(a) Inconsistency among the subsystems (b) Objective function

Fig. 6. Results obtained from the dynamic weight and the overall compatibility constraint.

problem. The optimization results obtained from the two cases (i.e., with the overall compatibility constraint adopted and not adopted) are compared.

Figs. 5(a) and (b) present the convergence curves for the system-level objective function and the inconsistency among the subsystems when the overall compatibility constraint is not adopted in the system level. Figs. 6(a) and (b) present the convergence curves for the system-level objective function and the inconsistency among the subsystems when the overall compatibility constraint is adopted in the system level.

Figs. 5(a) and 6(a) indicate that the interdisciplinary inconsistency curves converge to zero, and the interdisciplinary consistency requirements are satisfied. This phenomenon indicates that the proposed dynamic weight in the LPP model can guarantee the interdisciplinary consistency.

Fig. 5(b) illustrates that the solutions of the system-level objective function starting from points 2 and 4 are the worst with a value of 49.6552 and the best with a value of 5.4953, respectively. The maximum difference between these two solutions is 44.1599. Therefore, the solution of the system-level objective function is affected by the initial point when the overall compatibility constraint is not adopted in the system level.

Fig. 6(b) implies that the solutions of the system-level objective function starting from points 4 and 3 are the worst with a value of 6.0011 and the best with a value of 5.5942, respectively. The maximum difference between these two solutions is 0.4069, which is smaller than 44.1599 (i.e., the maximum difference obtained without the overall compatibility constraint in the system level). Therefore, the overall compatibility constraint should be adopted in the system level to reduce the influence of the starting point on the optimization result.

5. Conclusions

An improved MOCO strategy is presented for MDO problems with multi-objective subsystems. The LPP method is adopted to resolve the multi-objective subsystem optimization, and the weighted incompatibility function is added to the piecewise linear function of the LPP model. An expression of the dynamic weight in the LPP model is also presented according to the inconsistency among the subsystems. In the engineering example of the parameter design of the rolling mill stand, the dynamic weight dominates the fixed weight. The interdisciplinary consistency obtained from the dynamic weight satisfies the interdisciplinary consistency requirements, which demonstrates the effectiveness of the proposed dynamic weight in the LPP model.

From the perspective of interdisciplinary consistency, the incompatibility function is more important than the physical objectives in the multi-objective subsystem. This study provides an effective strategy when the LPP method is used. Some efforts are still required to provide a specific value for μ, using the requirements of interdisciplinary consistency. This limitation is a motivation for the further development of the proposed method. In fact, the method addressing the incompatibility function in the multi-objective subsystem is an important issue in future research when other multi-objective optimization algorithms are adopted.

Acknowledgment

This study is supported by the National Natural Science Foundation of China (Grant No. 51305073, 51305074). The authors appreciate the helpful comments and suggestions provided by the anonymous referees on an earlier version of this paper.

References

[1] M. M. Joly, T. Verstraete and G. Paniagua, Multidisciplinary design optimization of a compact highly loaded fan, *Structural and Multidisciplinary Optimization*, 49 (3) (2014) 471-483.

[2] M. Balesdent, N. Bérend, P. Dépincé and A. Chriette, A survey of multidisciplinary design optimization methods in launch vehicle design, *Structural and Multidisciplinary Optimization*, 45 (5) (2012) 619-642.

[3] C. H. Huang, J. Galuski and C. L. Bloebaum, Multi-objective pareto concurrent subspace optimization for multidisciplinary design, *AIAA Journal*, 45 (8) (2007) 1894-1906.

[4] K. S. Zhang, Z. H. Han and W. J. Li, Bilevel adaptive weighted sum method for multidisciplinary multi-objective optimization, *AIAA Journal*, 46 (10) (2008) 2611-2622.

[5] R. V. Tappeta and J. E. Renaud, Multiobjective collaborative optimization, *Journal of Mechanical Design, Transactions of the ASME*, 119 (3) (1997) 403-411.

[6] C. D. McAllister and T. W. Simpson, Multidisciplinary robust design optimization of an internal combustion engine, *Journal of Mechanical Design, Transactions of the ASME*, 125 (1) (2003) 124-130.
[7] C. D. McAllister, T. W. Simpson, K. Hacker, K. Lewis and A. Messac, Robust multiobjective optimization through collaborative optimization and linear physical programming, *10th AIAA/ISSMO Multidisciplinary Analysis and Optimization Conference*, Albany, NY, USA (2004) 2745-2760.
[8] C. D. McAllister, T. W. Simpson, K. Hacker, K. Lewis and A. Messac, Integrating linear physical programming within collaborative optimization for multiobjective multidisciplinary design, *Structural and Multidisciplinary Optimization*, 29 (3) (2005) 178-189.
[9] H. Y. Li, M. X. Ma and W. L. Zhang, Improving collaborative optimization for MDO problems with multi-objective subsystems, *Structural and Multidisciplinary Optimization*, 49 (4) (2014) 609-620.
[10] H. Z. Huang, Y. Tao and Y. Liu, Multidisciplinary collaborative optimization using fuzzy satisfaction degree and fuzzy sufficiency degree model, *Soft Computing*, 12 (10) (2008) 995-1005.
[11] H. Y. Li, M. X. Ma and Y. W. Jing, A new method based on LPP and NSGA-II for multiobjective robust collaborative optimization, *Journal of Mechanical Science and Technology*, 25 (5) (2011) 1071-1079.
[12] A. Vikrant and A. Shapour, A genetic algorithms based approach for multidisciplinary multiobjective collaborative optimization, *11th AIAA/ISSMO Multidisciplinary Analysis and Optimization Conference*, Portsmouth, VA, USA (2006) 630-646.
[13] R. Sébastien, D. Philippe and B. Fouad, Collaborative optimization of complex systems: a multidisciplinary approach, *International Journal on Interactive Design and Manufacturing*, 1 (4) (2007) 209-218.
[14] W. Hu, S. Azarm and A. Almansoori, New approximation assisted multi-objective collaborative robust optimization (new AA-McRO) under interval uncertainty, *Structural and Multidisciplinary Optimization*, 47 (1) (2013) 19-35.
[15] M. Li and S. Azarm, Multiobjective collaborative robust optimization with interval uncertainty and interdisciplinary uncertainty propagation, *Journal of Mechanical Design, Transactions of the ASME*, 130 (8) (2008) 1-11.
[16] B. Dandurand, P. Guarneri, G. M. Fadel and M. M. Wiecek, Bilevel multiobjective packaging optimization for automotive design, *Structural and Multidisciplinary Optimization*, 50 (4) (2014) 663-682.
[17] F. Mastroddi and S. Gemma, Analysis of Pareto frontiers for multidisciplinary design optimization, *Aerospace Science and Technology*, 28 (1) (2013) 40-55.
[18] F. F. Xiong, G. R. Sun, Y. Xiong and S. X. Yang, A moment-matching robust collaborative optimization method, *Journal of Mechanical Science and Technology*, 28 (4) (2014) 1365-1372.
[19] D. B. Meng, H. Z. Huang, Z. L. Wang, N. C. Xiao and X. L. Zhang, Mean-value first-order saddlepoint approximation based collaborative optimization for multidisciplinary problems under aleatory uncertainty, *Journal of Mechanical Science and Technology*, 28 (10) (2014) 3925-3935.
[20] I. Kroo, S. Altus, R. Braun, P. Gage and I. Sobieski, Multidisciplinary optimization methods for aircraft preliminary design, *5th AIAA/NASA/USAF/ISSMO Symposium on Multidisciplinary Analysis and Optimization*, Panama City Beach, FL, USA (1994) 697-707.
[21] A. Messac, S. M. Gupta and B. Akbulut, Linear physical programming: a new approach to multiple objective optimization, *Transactions on Operational Research*, 8 (10) (1996) 39-59.
[22] L. H. Cui, *Machine optimization design and application,* Northeastern University Press, Shenyang, China (1989).
[23] X. T. Bai and W. J. Li, Using cooperated optimization method to realize the designing optimization of complex mechanical system, *Journal of Machine Design*, 23 (3) (2006) 31-33.
[24] N. M. Alexandrov and R. M. Lewis, Analytical and computational aspects of collaborative optimization for multidisciplinary design, *AIAA Journal*, 40 (2) (2002) 301-309.
[25] J. Lin, Analysis and enhancement of collaborative optimization for multidisciplinary design, *AIAA Journal*, 42 (2) (2004) 348-36.

Haiyan Li received her B.S., M.S. and Ph.D. degrees in Control Theory and Control Engineering from the Northeastern University, China. She is currently an associate professor and master supervisor at the Computing Center, Northeastern University, China. Her main research interests include multidisciplinary design optimization and approximation algorithms. Her research works have been published in several international journals, such as the *Journal of Mechanical Science and Technology* and *Structural and Multidisciplinary Optimization*.